

W₅O₁₄ Nanowires**

By Maja Remškar,* Janez Kovac, Marko Viršek, Maja Mrak, Adolf Jesih, and Alan Seabaugh

We report on the synthesis of quasi-1D W₅O₁₄ crystals using NiI₂ as a growth promoter. Photoelectron spectroscopy revealed the metallic conductivity of the W₅O₁₄ nanowires, which was also confirmed by direct-transport measurements on a double-stranded nanowire. Scanning electron microscopy and transmission electron-diffraction data are correlated with details of crystal growth revealing the possible mechanism of the formation of this rarely synthesized phase, which was reported as a homogeneous phase only in 1978 by McColm et al., and in the meantime has been declared as a compound that is rare.

1. Introduction

The Magnéli phases^[1] are a homologous series of quite stoichiometric phases of transition metal suboxides with unusual composition, such as Mo₉O₂₆ and W₁₈O₄₉. They have similar structures as tungsten and molybdenum bronzes with a general formula of A_xMO₃; where A is an electropositive element, such as an alkali metal and M represents a transition metal. Both families are potentially of high technological interest for different applications. The intercalation of donor ions or oxide vacancies into the WO₃ host lattice causes a color change (electrochromic coloration) in the bronzes and suboxides, respectively, which is frequently coupled with a transition from the non-conductive WO₃ material into controlled gapped semiconducting oxides^[2–4] and even to metals.^[5] This effect is important for their use in optical devices, including light-emitting diodes and laser diodes, as well as in display devices and smart windows.^[6] In addition, sodium-doped Na_xWO₃ (*x* is ca. 0.05) shows high-temperature superconductivity with a *T_c* of ca. 90 K.^[7]

Recently, research on nanomaterials with their size-dependent and low-dimensional physical and chemical properties recalled the scientific attention to tungsten sub-oxides, which show high aspect ratios and promising physical properties on the nanoscale. Nanomaterials as compared to the correspond-

ing bulk compounds show greatly enhanced gas-sensing performance^[8] and improved photochromic effects,^[9] and, particularly, W₁₈O₄₉ nanowire arrays exhibit excellent field-emission characteristics.^[10] Some WO_{3–x} needle-like crystals can also serve as precursors for the synthesis of WS₂ nanotubes.^[11]

Reduction of WO₃, which is monoclinic at ordinary temperatures and tetragonal at temperatures above 983 K, leads to structural changes of the ReO₃-type structure by a crystal shear mechanism,^[12] where groups of edge-sharing WO₆ octahedra are arranged along some crystallographic planes (CS; shear planes). The areas between them consist of corner-sharing octahedra typical for the pristine WO₃ structure. At further reduction (*x* ≤ 0.13) the shear planes begin to interact and form equidistant crystalline phases with a defined structure, the so-called Magnéli W_{*n*}O_{3*n*–2} series, for example W₂₀O₅₈. Prolonged reduction destabilizes the shear planes causing the formation of pentagonal columns (PC) with equatorial edge-sharing WO₆ octahedra. Two such oxides have been identified: W₁₈O₄₉ and W₂₄O₆₈. Monoclinic W₁₈O₄₉ with the largest oxygen deficiency in the WO_{2.7}–WO₃ region is reported as the only oxide that can be isolated in a pure form, which is not the case for other tungsten sub-oxides.

W₅O₁₄ belongs to the W_{*n*}O_{3*n*–1} series, in which the higher members are represented by mixed tungsten oxides. Monophasic W₅O₁₄ was only obtained in the presence of very small concentrations of iron,^[13] so small that it was not clear whether iron is incorporated into the structure or not. The phase consisted of purple–blue fibers that appeared after a relatively long heating period (one week) at 1373 K. Longer heating periods (4 weeks) led to more fine fibers of the same phase. The unit cell was determined as tetragonal with parameters: *a* = 2.333 ± 0.001 nm, *c* = 0.3797 ± 0.0001 nm and with a *P42m* space group. The phase contains pentagonal and hexagonal tunnels at the peripheries of WO₆ pentagonal columns and is isostructural with Mo₅O₁₄, although without the superlattice cell that is typical for Mo₅O₁₄. Furthermore, both compounds differ in thermal stability. While Mo₅O₁₄ decomposes at temperatures above 803 K, the W₅O₁₄ compound continues to grow even at more than double that temperature. The W₅O₁₄ phase was reported as one of the sub-stoichiometric tungsten

[*] Prof. M. Remškar, Dr. J. Kovac, M. Viršek, Dr. M. Mrak, Dr. A. Jesih
Solid State Physics Department, Jozef Stefan Institute
Jamova 39, 1000 Ljubljana (Slovenia)
E-mail: maja.remskar@ijs.si

Prof. A. Seabaugh
Department of Electrical Engineering, University of Notre Dame
266 Fitzpatrick Hall, Notre Dame, IN 46556 (USA)

[**] The authors thank Prof. F. Lévy, EPFL, for useful discussion, M. Kocmur for technical assistance in the crystal growth, Dr. V. Nemanic for advices in building the pumping system, S. Sutar for SEM measurements of the electric devices, and Y. Yan for evaporation of the electric contacts. This work was financed by the Ministry of Higher Education, Science and Technology of the Republic of Slovenia and by the FOREMOST project of the European Union 6-th Framework Program under contract NMP3-CT-2005–515840.

oxides formed in fluidized bed reactions and was successfully converted into WS₂ nanotubes.^[14]

In this work, we report on a synthesis, where a mostly pure quasi-1D W₅O₁₄ phase is formed from the vapor phase at the relatively low temperature of 1009 K using NiI₂ as a growth promoter. Scanning electron microscopy (SEM) and transmission electron diffraction data are correlated with details of crystal growth revealing the possible mechanism of the formation of this rarely synthesized phase, which was reported as a homogeneous phase only in 1978 by McColm et al., and in the meantime has been declared as very rare, especially in thin layers.^[15] It has also been reported as a possible oxygen-deficient phase formed during laser deposition of polycrystalline WO₃.^[16] Photoelectron spectroscopy revealed metallic conductivity of the W₅O₁₄ nanowires, which was confirmed also with direct transport measurements on a double stranded nanowire, which is important for their use in nanoelectronics.

2. Results

2.1. Scanning Electron Microscopy

The light-blue fibers representing only a few weight percentage of the transported material grew on the top of WS₂ platelets (Fig. 1a). The size distribution of the fibers with average diameter of 100 nm and lengths extending up to several hundreds of

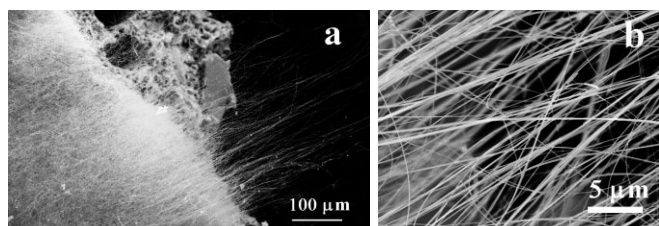


Figure 1. SEM images of a) the W₅O₁₄ nanowires grown on the WS₂ platelets. b) Very rigid W₅O₁₄ wires of an average diameter of 100 nm.

micrometers and even up to a few millimeters, depends on the growth conditions, namely, on the dynamic partial pressures of sulfur, water, iodine, nickel, and oxygen. There is a very narrow range of these parameters that are suitable for the successful growth of pure W₅O₁₄ nanowires. This together with the right selection of the transition metal promoting the growth at relatively low temperatures, explain why this phase was not synthesized as a homogeneous material until now. The wires grow in a rigid straightforward way (Fig. 1b) and show a large stability against tensile forces in accordance with the report of Frey et al.^[14]

2.2. X-ray Diffraction

The nanowires were examined by X-ray diffraction (XRD) and the positions of the diffraction peaks are in good agreement with the JCPDS-71-0292 file for W₅O₁₄ (Fig. 2). Because of the high aspect ratio of the fibers and the preferential orien-

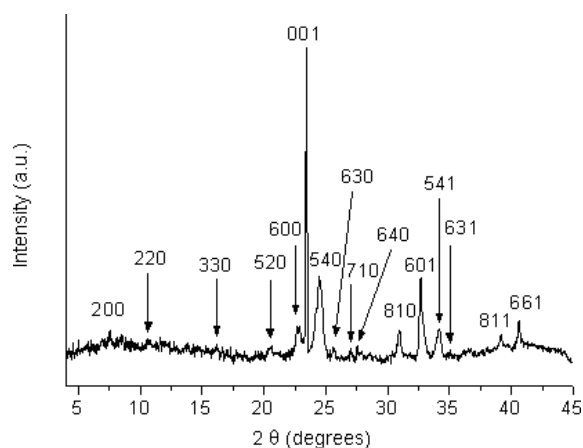


Figure 2. X-ray diffraction pattern of the tungsten oxide nanowires. Miller indices of the tetragonal W₅O₁₄ phase (JCPDS 71-0292, unit cell: $a = 2.333$ nm, $c = 0.3797$ nm) are indicated.

tation because of self-assembly in the sample, which was inserted into a 0.3 mm capillary, the relative intensities can not be used as an accurate reference for comparison. Nevertheless, the strongest peaks corresponding to the 0.379 nm and 0.363 nm interlayer distances accurately match the most intensive (001) and (540) peaks for the reported W₅O₁₄ phase.^[13]

2.3. Transmission Electron Microscopy and Diffraction

Figure 3 shows high-resolution transmission electron microscopy (TEM) images and diffraction patterns of a single W₅O₁₄ fiber. The needle crystals grow in the longitudinal direction

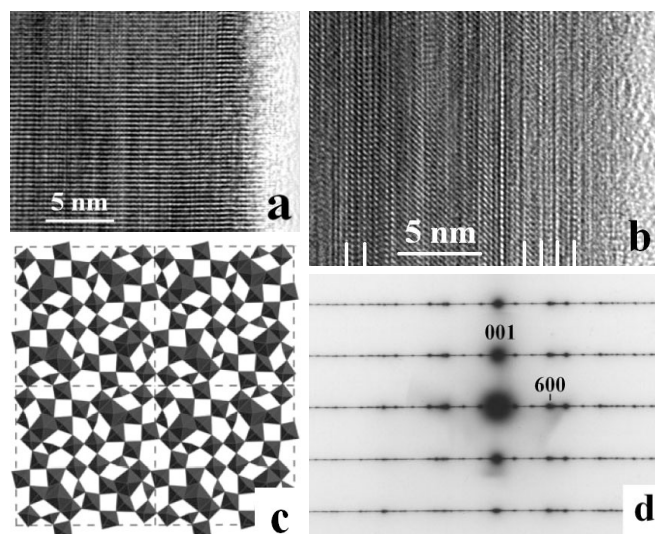


Figure 3. High-resolution TEM and electron diffraction of the W₅O₁₄ nanowires: a) the (001) planes perpendicular to the needle axis with the interlayer distance of $0.366(1 \pm 0.05)$ nm; b) the [010] zone with the intensity modulation with periodicity of $1.14(1 \pm 0.02)$ nm, marked with white lines; c) a schematic representation of W₅O₁₄ in the [001] direction with a network of hexagonal and pentagonal columns [15], the transmission electron diffraction of the [010] zone of the W₅O₁₄ wires with the [001] direction parallel to the wire's longitudinal axis.

along the [001] crystallographic axis. The (001) planes are distributed in defect-free order (Fig. 3a) with an interlayer distance of $0.366(1 \pm 0.05)$ nm, which corresponds to the (001) interlayer distance of the W₅O₁₄ phase (0.3797 nm, JCPDS-71-0292).^[13] The intensity modulation along the fiber length superimposes and blurs the (100) fringes separated by $0.4(1 \pm 0.03)$ nm, which corresponds to the (600) planes of the W₅O₁₄ compound (0.38883 nm). The [010] zone of the W₅O₁₄ crystal (Fig. 3b) reveals the origin of the intensity modulation in the peculiar structure of the lattice. The modulation with periodicity of $1.14(1 \pm 0.02)$ nm (marked with white lines) agrees perfectly with half the unit cell parameter along the [100] axis (2.233 nm), which confirms the regular modulation of the electron density in accordance with the model structure of W₅O₁₄ (Fig. 3c).^[14]

The transmission electron diffraction by a single nanowire (Fig. 3d) shows the [010] zone of W₅O₁₄ with the [001] direction parallel to the longitudinal axis of the wire, and the [100] one that is perpendicular to it. Contrary to the inaccuracy of the X-ray diffraction intensities, the relative intensities of the (200), (400), (600), and (800) electron-diffraction spots agree well with the intensities reported for the W₅O₁₄ phase^[13] as well as with the intensity modulation observed by HRTEM

(Fig. 3b). The strongest (600) peak corresponds to the size of the unit cell in the [100] direction.

2.4. Photoelectron Spectroscopy

The photoelectron spectra of the W₅O₁₄ nanowires (Fig. 4) were measured using an analytical surface of 0.4 mm in diameter and a depth sensitivity of $3\text{--}5$ nm. In this way large numbers of nanowires could be analyzed at the same time. The monochromatic Al X-ray source used for excitation and pass energy of the electron analyzer yielded an overall energy resolution in the XPS spectra of 0.6 eV measured at the Ag $3d_{5/2}$ peak. The binding-energy scale was checked by the C $1s$ peak at 284.6 eV originating from adsorbed molecules. It is worth to note that no charging was observed in the XPS spectra suggesting a conductive nature of the analyzed nanowires. In addition, we did not find any indication of iodine presence in the nanowires.

For tungsten a complex energy distribution of W $4f$ photoelectrons was obtained as shown in Figure 4a. The W $4f$ spectrum was fitted with six components, associated with two different oxidation states of the W atoms. The peaks at 36.1 eV, 38.2 eV and 42.0 eV represent emission from W $4f_{7/2}$, $4f_{5/2}$, and $5p_{3/2}$ core levels from the W atoms in the $6+$ oxidation state.

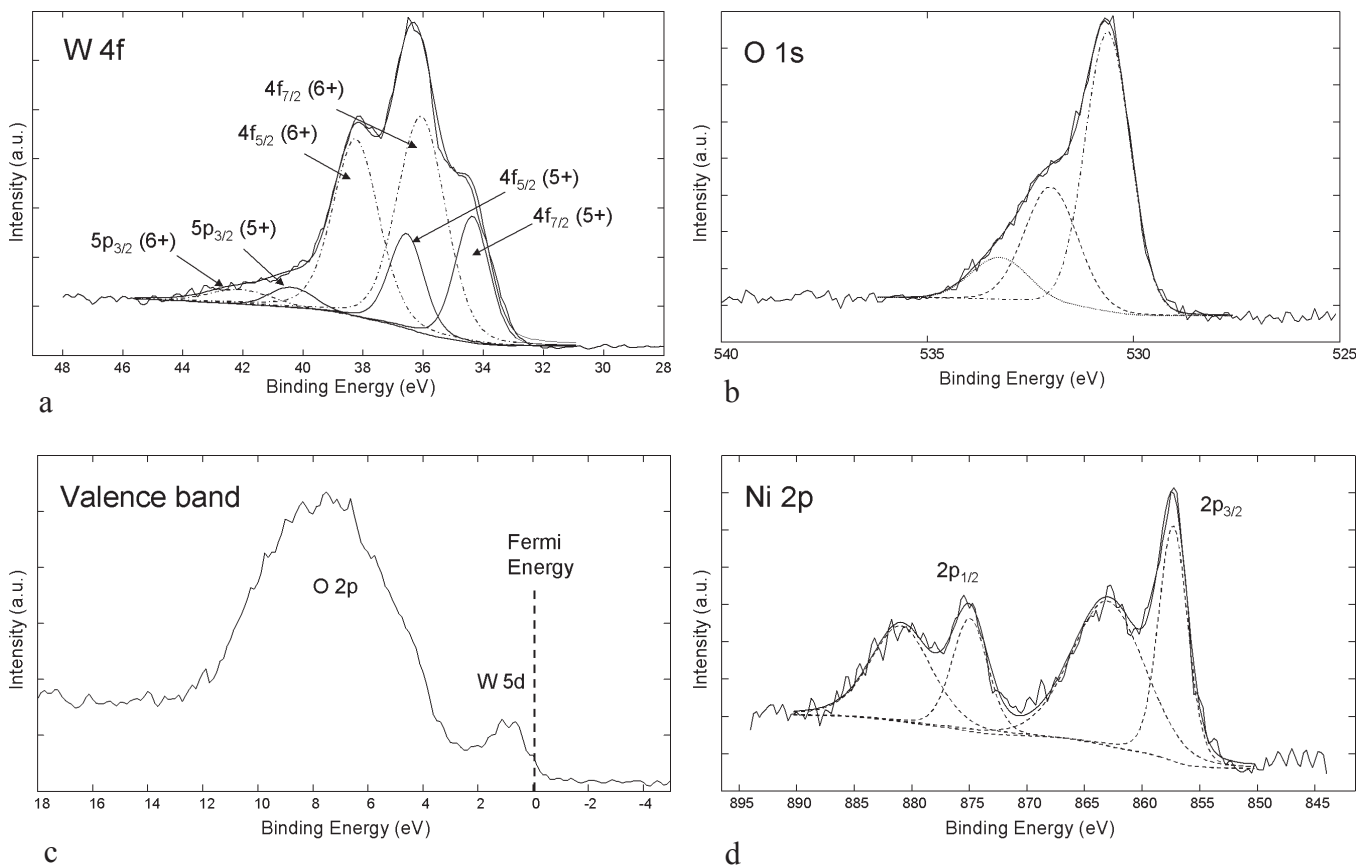


Figure 4. XPS spectra of the W₅O₁₄ nanowires: a) high-energy resolution W $4f$ core-level spectrum with peaks corresponding to $6+$ and $5+$ oxidation numbers; b) spectrum of O $1s$ photoelectrons revealing the contribution from bonds with tungsten in an oxidation state lower than $6+$; c) the W $5d$ conduction band with states at the Fermi level revealing the metallic conductivity of the nanowires; d) the Ni $2p$ core-level spectrum associated with the Ni(OH)₂ compound.

The peaks at 34.4 eV, 36.6 eV, and 40.2 eV result from emission from the W 4f_{7/2}, 4f_{5/2}, and 5p_{3/2} core levels from the W atoms in the oxidation state that has been attributed to the 5+ or to the W-suboxide state in the literature on flat tungsten oxides.^[16,17] No W 4f peaks that can be attributed to W⁴⁺ (33.3 and 35.5 eV) or metallic tungsten (31.2 eV, 33.4 eV)^[15] were observed.

The two oxidation numbers (6+ and 5+) evidence that besides the tungsten coordination that is typical for the ReO₃ structural type (WO₃ with W⁶⁺) there is also a non-negligible number of tungsten atoms coordinated by shared oxygen atoms as it is typical for the CS and PC structures. Each W atom in the CS plane has the oxidation number 5+, while the W atoms of the PC structure have an average oxidation number of 5.34+. One unit cell of the W₅O₁₄ structure contains 4 PC and 15 corner-shared WO₃ octahedra, which on average corresponds to the oxidation number of 5.6+.

The photoelectrons from O 1s (Fig. 4b) form a relatively wide and asymmetric peak with the highest point at 530.6 eV, which corresponds to the oxygen bond with W⁶⁺ (O²⁻) in WO₃. The other two peaks at the higher photoelectron energies of 532.0 eV and 533.2 eV and can be attributed to the bonds with tungsten in lower oxidation states and/or to C–O bonds originating from adsorbed molecules.

The valence-band spectrum (Fig. 4c) shows the structure beneath the Fermi energy with a maximum at about 0.5 eV. We relate this structure to the W 5d orbitals. Its position means that a conduction band is formed in the W₅O₁₄ nanowires which results in metallic behavior. The W 5d peak is superimposed onto the broad peak associated with the O 2p–W 5d orbitals with its maximum around 7 eV.

A weak Ni 2p signal was also detected in the XPS spectrum (Fig. 4d). We believe that it originates from nickel that is trapped between bundles or on the surface of the W₅O₁₄ nanowires, especially at their longitudinal terminations. The binding energy of the Ni 2p_{3/2} peak at 857.3 eV and the pronounced satellite structure at 862.5 eV indicate that the Ni 2p signal can be related to a Ni(OH)₂ compound.^[18]

2.5. Transport in a Single W₅O₁₄ Nanowire

Two and three-terminal devices were fabricated from W₅O₁₄ nanowires. The wires were placed on a thermally oxidized, heavily doped p-Si substrate. Aluminum contacts 1 μm in thickness were formed by electron-beam evaporation through stencil masks with approximately 150 μm diameter apertures. Two-terminal measurements showed metallic (ohmic) conduction in the nanowires. No photoconductivity was observed between measurements made in the dark and under strong microscope illumination using a halogen lamp. The wire conductivity could not be modulated when backgated through the p+ Si substrate in the range from –2 to +2 V with a tube bias ranging from 0 to 2 V, consistent with a metallic tube. Placement of three contacts along a double-stranded nanowire with a length exceeding 600 μm has allowed the measuring of the specific resistivity of the W₅O₁₄. Shown in Figure 5 is a measurement of the double-stranded wire resistance obtained by ramping the current through the nanowires end-to-end while measuring the potential difference at two

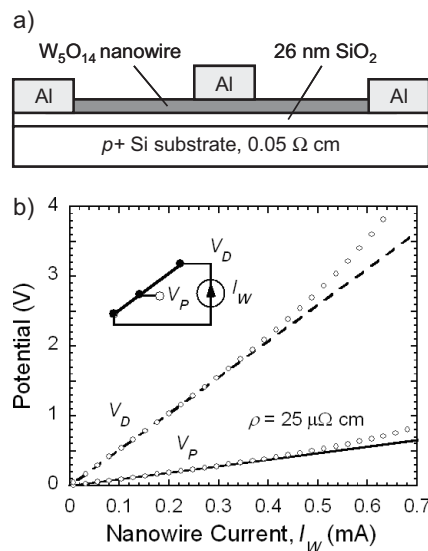


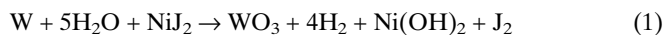
Figure 5. Transport measurement in a single W₅O₁₄ nanowire: a) Schematic cross section of a three-terminal nanowire. b) Potential versus tube current for a 600 μm long double-stranded nanowire (120 nm and 155 nm in radius) with two 150 μm diameter Al contacts connecting the tube at either end and another contact touching the tube along its length.

places along the tube as shown schematically in the inset of Figure 5. The voltage at V_D is the sum of the potential drop across the tube plus the voltage drop across the contacts at either end. The measurement at V_P eliminates one of these contact resistances and allows the characterization of the maximum resistivity of the wire given the measured wire length and diameters (by scanning electron microscopy). The nanowire resistivity obtained in this way is 25 Ω cm.

3. Discussion

The dynamic and complex growth conditions, especially the hydrogen and H₂S partial pressures, which both have a reducing effect at high-temperature annealing, and the role of nickel and iodine in the process, all these parameters make the understanding of the growth mechanism difficult. It was experimentally confirmed that the W₅O₁₄ nanowires did not grow in the absence of nickel. At the hot zone (1123 K) WS₂ was decomposed and tungsten reacting with iodine was transported to the growth zone (1010 K) of the ampoule. NiI₂ with melting and boiling temperatures at 1053 K and 1070 K, respectively, was found in the vapor phase. Intermediate nickel, sulfur, and/or water reactive products, such as Ni(OH)₂, NiSO₄, or different NiS_z compounds, are expected, but when the reaction was finished, only the Ni(OH)₂ phase was confirmed by XPS. Water vapor is the obvious oxygen source, but it is not a question of a simple exchange from the starting material as there is also a need for hydrogen in the reaction, which reacts with sulfur to reduce WO₃ to W₅O₁₄. The rare brittle crystals of the W₁₈O₄₉ phase, which has the largest oxygen deficit with regard to stoichiometric WO₃, terminate the growth process of the oxides.

Sulfur is left as the reduction product and is used in the growth of some quasi-spherical groups of WS₂ platelets nucleated on the surface of the W₅O₁₄ nanowires. We postulate the following reaction schemes for the formation of the W₅O₁₄ nanowires:



One can speculate about the role of nickel, but we have evidenced that the homogeneous W₅O₁₄ phase did not grow in diminishing nickel atmosphere. Compared to the report of the iron-promoted growth of W₅O₁₄,^[13] where the concentration of iron in W₅O₁₄ was below the detection limit, we propose a rheotaxy role of nickel hydroxide in the growth process, most probably at the interface between the WS₂ plate-like base and the sub-oxide needles or at the terminations of the oxide needles. It is known that nickel efficiently anneals pentagonal defects during the growth of carbon nanotubes and in such a way prevents the dome closure of the tubes, which stops their longitudinal growth.^[19] In the WS₂-nickel system it was found that nickel delivers the nucleation seeds for the WS₂ crystallites resulting in better WS₂ orientation and adhesion on the SiO₂/Si(100) substrate in the sputtered thin films. The formed NiS_x interfacial layer promotes film crystallization at temperatures above its melting point through enhanced mobility in a rheotaxy process.^[20]

It is reasonable to predict a similar role in the growth mechanism of W₅O₁₄ crystals. In this case the formed Ni(OH)₂ interfacial layer with its melting temperature of 503 K serves as the growth promoter. The enhanced mobility of tungsten atoms through the Ni(OH)₂ phase from the WS₂ base or transported by the gas phase explain the very fast longitudinal growth after the initial nucleation, as well as the observation that the needles were always found on the top surface of the transported layered crystals. The same mechanism (with a Fe(OH)₂ enhanced diffusion layer) can also be used to interpret the growth of the iron-promoted W₅O₁₄ phase synthesized nearly 30 years ago.

4. Conclusions

W₅O₁₄ nanowires have been synthesized by a chemical-transport technique using nickel as a growth promoter. The crystals show a high mechanical strength and grow up to several millimeters in lengths and up to 200 nm in width. We have managed to prepare this rarely synthesized phase as a highly homogeneous and chemically stable material. The transport measured in a single nanowire revealed metallic conductivity with a specific resistivity of 25 μΩ cm. The XPS measurements confirmed metallic conductivity of the nanowires and revealed different oxidation states of tungsten in accordance with the model structure containing pentagonal columns. The growth

mechanism is proposed explaining the importance of sulfur and water in the process. The presence of nickel was found to be crucial for the formation of the W₅O₁₄ nanowires, because the Ni(OH)₂ phase situated at the interface between the WS₂ plate-like base and the sub-oxide needles enables fast tungsten diffusion, which leads to a highly anisotropic growth. The well-ordered nanoporous structure with hexagonal tunnels, which can serve as diffusion paths for foreign intercalated species make this material technologically very promising.

5. Experimental

We have prepared the W₅O₁₄ nanowires by an iodine (99.8%, Sigma-Aldrich) transport method from 0.60 g WS₂ (powder, 99%, Sigma-Aldrich) adding 0.0678 g of NiI₂ (powder, nickel(II) iodide, Sigma-Aldrich), and 20 μL of distilled H₂O. The transport reaction was running for 2–3 weeks in an evacuated silica ampoule at a pressure of 5 × 10⁻⁵ Pa. The material was transported from the source (hot zone at 1123 K) to the growth zone (1009 K), with a temperature gradient of 5.7 K cm⁻¹, by iodine in a volume fraction of 3.2 mg cm⁻³ that was used as the transport agent. The so-produced nanowires were studied using transmission electron microscopy (200 keV Jeol 2010F), scanning electron microscopy (FE-SEM, Supra 35 VP, Carl Zeiss), X-ray diffraction (Siemens D-5000), and photoelectron spectroscopy (XPS, Physical Electronics Inc, TFA XPS), while the transport in the nanowires was measured using an Agilent 4155 semiconductor parameter analyzer.

Received: November 29, 2006

Revised: April 4, 2007

Published online: July 4, 2007

- [1] L. Kihlberg, I. Olovsson, *Acta Cryst.* **1997**, A53, 103.
- [2] G. Du, Q. Chen, R. Che, Z. Yuan, L. Peng, *Appl. Phys. Lett.* **2001**, 79, 3702.
- [3] H. Cheng, Y. Chen, H. Lin, C. Mou, *Appl. Phys. Lett.* **2001**, 78, 3791.
- [4] V. Srikant, D. R. Clarke, *J. Appl. Phys.* **1998**, 83, 5447.
- [5] W. R. Gardner, G. C. Danielson, *Phys. Rev.* **1954**, 93, 46.
- [6] M. S. Wittingham, in *Recent Advances in Fast Ion Conducting materials and Devices* (Eds: B. V. R. Chowdary, Q. G. Liu, L. Q. Chen), World Scientific, Singapore **1990**.
- [7] A. Shengelaya, S. Reich, Y. Tsabba, K. A. Muller, *Eur. Phys. J. B* **1999**, 12, 13.
- [8] J. L. Solis, S. Saukko, L. Kish, C. G. Granqvist, V. Lantto, *Thin Solid Films* **2001**, 391, 255.
- [9] S. T. Li, M. S. El-Shall, *Nanostruct. Mater.* **1999**, 12, 215.
- [10] Y. B. Li, Y. Bando, D. Goldberg, *Adv. Mater.* **2003**, 15, 1294.
- [11] A. Rothschild, J. Sloan, R. Tenne, *J. Am. Chem. Soc.* **2000**, 122, 5169.
- [12] A. Polaczek, M. Pekala, Z. Obuszko, *J. Phys. Condens. Matter* **1994**, 6, 7909.
- [13] I. J. McColm, R. Steadman, S. J. Wilson, *J. Solid State Chem.* **1978**, 23, 33.
- [14] G. L. Frey, A. Rothschild, J. Sloan, R. Rosentsveig, R. Popovitz-Biro, R. Tenne, *J. Solid State Chem.* **2001**, 162, 300.
- [15] M. Katoh, Y. Takeda, *Jpn. J. Appl. Phys.* **2004**, 43, 7292.
- [16] F. Bussolotti, L. Lozzi, M. Passacantando, S. La Rosa, S. Santucci, L. Ottaviano, *Surf. Sci.* **2003**, 538, 113.
- [17] J. F. Moulder, W. F. Stickle, P. E. Sobol, K. D. Bomben, in *Handbook of X-Ray Photoelectron Spectroscopy*, Physical Electronics Inc., Eden Prairie, MN **1995**.
- [18] A. N. Mansour, *Surf. Sci. Spectra* **1996**, 3, 239.
- [19] Y. H. Lee, S. G. Kim, D. Tomanek, *Phys. Rev. Lett.* **1997**, 78, 2393.
- [20] C. Ballif, M. Regula, P. E. Schmid, M. Remskar, R. Sanjinés, F. Lévy, *Appl. Phys. A* **1996**, 62, 543.